Radiochim. Acta **92**, 757–763 (2004)
© by Oldenbourg Wissenschaftsverlag, München

In-situ diffusion of HTO, $^{22}Na^+$, Cs^+ and I^- in Opalinus Clay at the Mont Terri underground rock laboratory

By L. R. Van Loon[1,*], P. Wersin[2], J. M. Soler[3], J. Eikenberg[1], Th. Gimmi[1], P. Hernán[4], S. Dewonck[5] and S. Savoye[6]

[1] PSI, CH-5232 Villigen, Switzerland
[2] NAGRA, CH-5430 Wettingen, Switzerland
[3] CSIC-IJA, E-08028 Barcelona, Spain
[4] ENRESA, E-28043 Madrid, Spain
[5] ANDRA, F-55290 Bure, France
[6] IRSN, F-92265 Fontenay-aux-Roses, France

(Received August 18, 2003; accepted March 9, 2004)

In situ diffusion / Opalinus Clay / Mont Terri / Radionuclides / Modelling

Summary. The diffusion properties of the Opalinus Clay were studied in the underground research laboratory at Mont Terri (Canton Jura, Switzerland) and the results were compared with diffusion data measured in the laboratory on small-scale samples. The diffusion of HTO, $^{22}Na^+$, Cs^+ and I^- were investigated for a period of 10 months. The diffusion equipment used in the field experiment was designed in such a way that a solution of tracers was circulated through a sintered metal screen placed at the end of a borehole drilled in the formation. The concentration decrease caused by the diffusion of tracers into the rock could be followed with time and allowed first estimations of the effective diffusion coefficient. After 10 months, the diffusion zone was overcored and the tracer profiles measured. From these profiles, effective diffusion coefficients and rock capacity factors could be extracted by applying a two-dimensional transport model including diffusion and sorption. The simulations were done with the reactive transport code CRUNCH. In addition, results obtained from through-diffusion experiments on small-sized samples with HTO, $^{36}Cl^-$ and $^{22}Na^+$ are presented and compared with the *in situ* data. In all cases, excellent agreement between the two data sets exists. Results for Cs^+ indicated five times higher diffusion rates relative to HTO. Corresponding laboratory diffusion measurements are still lacking. However, our Cs^+ data are in qualitative agreement with through-diffusion data for Callovo–Oxfordian argillite rock samples, which also indicate significantly higher effective diffusivities for Cs^+ relative to HTO.

1. Introduction

Argillaceous formations are considered as potential host rocks for radioactive waste disposal in a number of countries [1–3]. The main reason for this is the very low permeability of such formations, which make them ideal containments for isolating radioactive contaminants for very long time periods. The main process responsible for possible transport of radionuclides in such formations is molecular diffusion. It is therefore very important to know the diffusion behaviour of radionuclides in these argillaceous formations. It is common practice to study diffusion on small-scale samples in the laboratory [4–6]. However, to what extent the results of such studies can be extrapolated to field situations is unclear, and therefore it is also important to study diffusion *in-situ* and to compare the results with lab diffusion data. Finally, data on isotope profiles in the formations [7, 8] can be used to build up confidence in using short term, small-scale data to predict large scale, long-term processes.

A preliminary *in situ* migration experiment (DI) with non-reactive tracers (HTO, I^-) was performed for a period of one year [6, 9, 10] and showed the feasibility of performing *in-situ* diffusion experiments. The effective diffusion coefficient (D_e) for tritium extracted from the *in situ* diffusion test was about 5×10^{-11} m^2 s^{-1} for diffusion parallel to the bedding plane, which is comparable with the value of $(5.4 \pm 0.4) \times 10^{-11}$ m^2 s^{-1} measured in the laboratory [11]. Diffusion of iodide in the DI experiment, however, was not consistent with laboratory data, suggesting that a retardation and/or oxidation process had occurred in the borehole or the rock [6].

The long-term diffusion experiment presented in this study (DI-A) aims at understanding the diffusion behaviour of radionuclides in the Opalinus Clay [12]. The main focus lies on the diffusion of sorbing species which, so far, have not been studied at Mont Terri. Besides the non-sorbing tracers HTO and I^- which were injected for comparison reasons with the previous DI experiment, the diffusion of the weakly and more strongly sorbing elements, $^{22}Na^+$ and Cs^+ respectively, was investigated. The field investigations were complemented by diffusion experiments parallel to the bedding plane performed in the laboratory. This study presents the second part of the DI-A *in-situ* experiment and, for comparison, the data from through-diffusion measurements. The first part of the experiment has been already published elsewhere [12].

2. Experimental procedures

2.1 Experimental set-up

The geologic setting and the layout of the experiment have been described in detail by Wersin *et al.* [12]. A schematic

*Author for correspondence (E-mail: luc.vanloon@psi.ch).

source: https://doi.org/10.7892/boris.47691 | downloaded: 22.6.2024

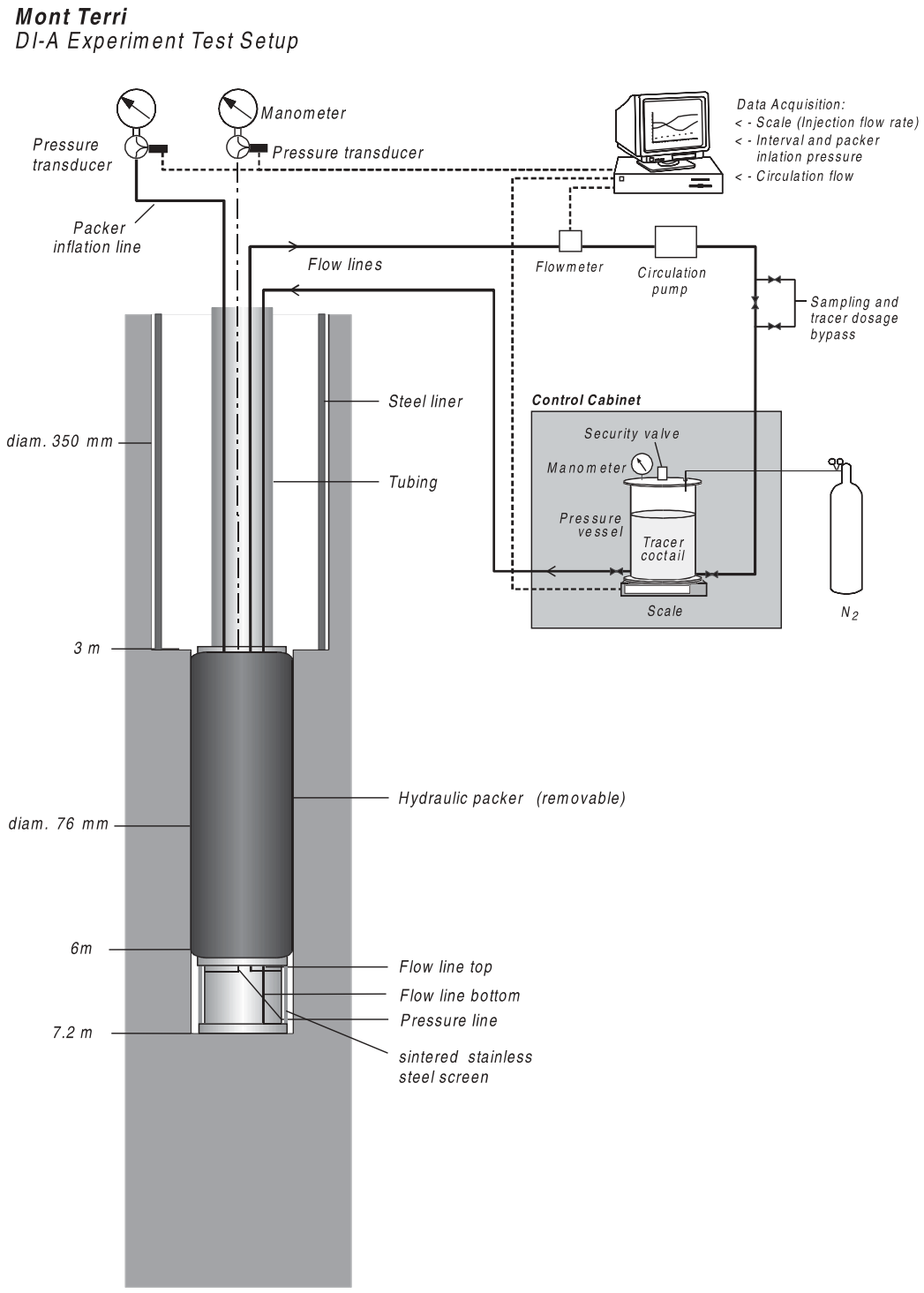

Fig. 1. Layout of the diffusion experiment (DI-A), showing main features of the downhole and surface equipment.

view of the experiment is depicted in Fig. 1. A borehole was equipped with a single packer and a sintered stainless steel filter of 1 m length. The test interval has a diameter of 76 mm and is hydraulically isolated between a depth of 7.20 and 6.20 m. Two flow lines made of stainless steel, and a magnetic gear pump enable water and tracer circulation in the test interval. The water used was a synthetic Opalinus Clay (OPA) pore water [13]. The tracers injected in the borehole were Cs^+, I^-, $^{22}Na^+$ and HTO. After tracer injection, the concentration and/or radioactivity in the borehole solution was monitored by regularly sampling aliquots of the circulating fluid.

2.2 Overcoring

After 292 days of diffusion time, the equipment was retrieved and the single packer removed from the borehole. Then the lower 4 metres of the borehole were immediately filled with a quartz/resin mixture to stabilise it. The test interval was then overcored with a double core barrel containing a steel liner of 290 mm outer diameter (inner diameter = 234 mm). The overcoring borehole was drilled to a depth of 7.87 m without removing the core sections from the borehole. After 7.87 m was reached, the entire core was lifted and cut into core sections of about 1 m length at the bore-

hole mouth. Each core section was packed in a steel liner. More details of the overcoring procedure can be found in Möri *et al.* [14].

2.3 Sampling

The aim of sampling was to extract undisturbed rock samples from the overcore in order to get concentration profiles of the different isotopes. After removing, the overcore was reorientated with the help of the well-known orientation of the bedding planes and a reference line was drawn on the surface of the uncovered core. Then the exact depth position of the overcore containing the test interval was localised.

The drilling equipment consists of a Hilti drilling machine with a 51 mm single core barrel. Dry drilling was performed at low speed to avoid heating of the core. The barrel was connected to a vacuum cleaner to remove dust, and to cool the equipment and the drillcore. The drillcores were sliced into wheels of 1 cm thickness and the partly desaturated surface of the small diameter drill cores was cut away with a saw (Fig. 2).

Nine profiles were sampled from the overcore. Each sample profile was defined by the location of the profile origin and the orientation of the profile [14].

2.4 Analyses

The rock samples were immediately transferred into 50 cm^3 polyethylene bottles and the weight (rock + pore water) measured on an analytical balance (Mettler Toledo, Type PR503, accuracy ± 0.01 g). About the same quantity of de-ionised water was then added, the weight measured again, and the bottles closed and shaken on a shaking table. Addition of 30 g water to 20 g solid material proved to be sufficient for disaggregating the clay in less than one hour. After disaggregation, the samples were centrifuged at $10\,000 \times$ g for 30 minutes to obtain a phase separation. The clear supernatant and the solid phase were used for further analysis.

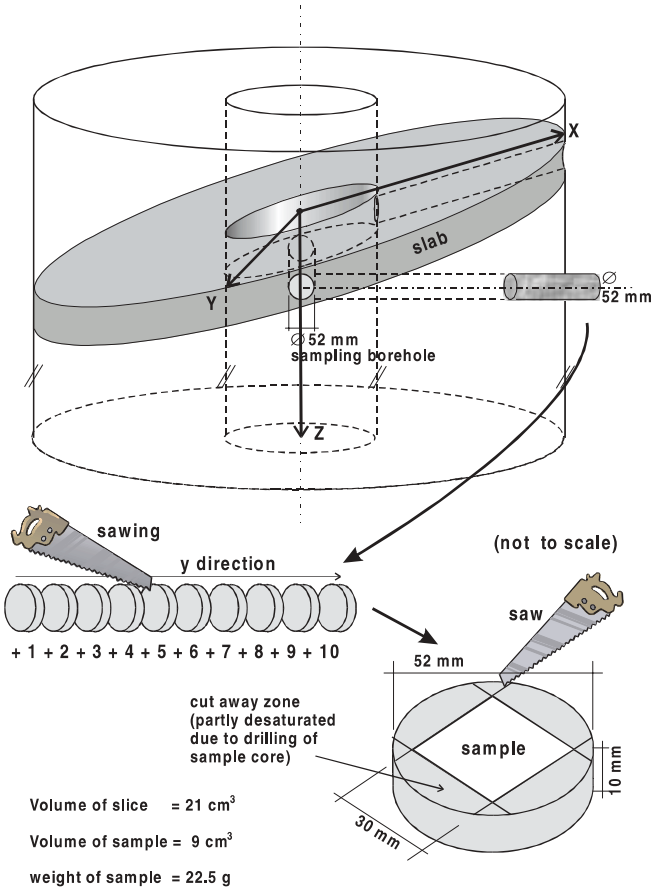

Fig. 2. Sampling of the profile.

2.4.1 HTO

HTO was measured by liquid scintillation counting (TriCarb 2770 super low level, Packard-Canberra; counting window 0–8 keV). 10 ml of the supernatant were mixed with 10 ml of a scintillation cocktail (Ultima Gold LLT). Spillover from ^{22}Na into the energy window of HTO could be omitted because the HTO-activities of each sample were at least one order of magnitude higher than those of ^{22}Na.

2.4.2 Sodium

^{22}Na in the liquid phase was measured *via* γ-spectrometry and *via* liquid scintillation counting (counting window 8–800 keV). The remaining fraction of ^{22}Na in the solid phase was measured *via* γ-spectrometry using a high resolution intrinsic *p*-type coaxial Ge-detector (Princeton gamma Tech, PGT, model IGC30). Spectrum analysis and peak deconvolution were performed automatically using Interwinner 5.1 software (EG&G Ortec).

2.4.3 Iodide

Iodide was analysed using ion chromatography (Dionex DX 120; AS14A column; AG14A precolumn; Atlas AAES conductivity suppressor). The eluent used was a 8.0 mM Na_2CO_3/1 mM $NaHCO_3$ buffer (flow rate: 1 $cm^3\,min^{-1}$).

2.4.4 Caesium

Only a few selected samples were analysed for caesium (profile 1, 2 and 3). OPA samples (~ 1 cm^3) were ground and sieved through a 63 μm size sieve. Prior to the extraction procedure, the water content of the OPA samples was determined by heating at 105 °C until constant weight. The water content was 2.18 wt. % (average value of 6 measurements). 3 grams of OPA samples were weighed in 40 ml polypropylene tubes and 30 ml of a 1 M KNO_3 was added. (The S : L ratio ~ 0.1 kg L^{-1}.) Suspensions were end-over-end shaken for 3 days. Phase separation was carried out by centrifugation (1 hour at $96\,000 \times$ g). The clear supernatant solutions were analysed for Cs by AAS (IL951 AA/AE Spectrophotometer, Instrumentation Laboratory Inc., USA). The pH of the supernatant solutions was 8.1 ± 0.1. Extractions were carried out in air atmosphere.

Comparison with X-ray fluorescence spectrometry (XRF) analysis (PSI, unpublished data) indicated that about 70% of total Cs is extracted by the KNO_3-method.

Bereitgestellt von | Universitätsbibliothek Bern
Angemeldet | 130.92.9.56
Heruntergeladen am | 12.05.14 12:00

3. Results and discussion

3.1 Model description

The results from the field experiment have been interpreted by means of two-dimensional transport calculations including diffusion and sorption. The concept behind these calculations is that transport is dominated by diffusion along the bedding planes (preferential fast pathways for diffusion). The reactive transport code CRUNCH has been used for the simulations. CRUNCH is the latest evolution of the GIMRT/OS3D software package [15, 16].

The equation of conservation of mass for a given tracer can be written as

$$\frac{\partial c_{\mathrm{tot}}}{\partial t} = \nabla(D_{\mathrm{e}} \nabla c)\,, \tag{1}$$

where c is concentration in solution [moles per volume of solution], t is time [s], D_{e} is the effective diffusion coefficient [$\mathrm{m^2\,s^{-1}}$], ϕ is the accessible porosity for the tracer and c_{tot} is the total concentration of tracer [moles per bulk volume], which is given by

$$c_{\mathrm{tot}} = \phi c + \rho_{\mathrm{d}} s\,, \tag{2}$$

where ρ_{d} is the bulk dry density [$\mathrm{kg\,m^{-3}}$] and s is the concentration of tracer sorbed on the solids [moles per mass of solid]. Three types of sorption models have been implemented, corresponding to (a) $s = 0$ (non-sorbing tracer), (b) $s = K_{\mathrm{d}} c$ (linear sorption), or (c) $s = a c^b$ (Freundlich isotherm). Radioactive decay is not explicitly included in the calculations. Instead, the experimental concentrations of HTO (non-sorbing) and $^{22}Na^+$ (linear sorption) are corrected for decay before comparing with modelling results.

The geometry of the problem is schematically shown in Fig. 3. The calculation domain corresponds to a bedding plane. The fact that the bedding is at an angle (45°) with respect to the borehole is taken into account by the elliptical shape of the borehole (intersection of bedding and borehole). All the boundaries of the domain are no-flux boundaries. The initial conditions are

Borehole: $c(x, y, t = 0) = c_{\mathrm{tot}}(x, y, t = 0) = c_0\,,$

Rock: $c_{\mathrm{tot}}(x, y, t = 0) = c_{\mathrm{back}}\,,$

where c_0 is the initial concentration in the injection system and c_{back} is the background concentration of the tracer in the Opalinus Clay ($c_{\mathrm{back}} = 0$ for HTO and $^{22}Na^+$; c_{back} equals a small number for I^- and Cs^+). Only one quarter of the two-dimensional system is taken into account in the calculations due to symmetry considerations (diffusion is assumed to be homogeneous and isotropic along the plane). A large value of D_{e} is assumed in the borehole, in order to maintain a homogeneous concentration (well mixed conditions in the injection system). The total volume of solution in the injection system (about 11 $\mathrm{dm^3}$) is also taken into account.

3.2 Modelling results

The results of model calculations are compared with the evolution of tracer concentrations in the injection system and the measured tracer profiles in the rock around the borehole. Fitting both tracer concentrations in the injection system and in the rock profiles provides a unique set of effective diffusion coefficients (D_{e}) and porosity/sorption values (rock capacity factors in the case of linear sorption). As shown below, the agreement between model and measured profiles is better for the profiles measured directly along bedding planes than for profiles measured at an angle with respect to bedding (profiles at an angle have been projected onto a bedding plane for comparing with model calculations).

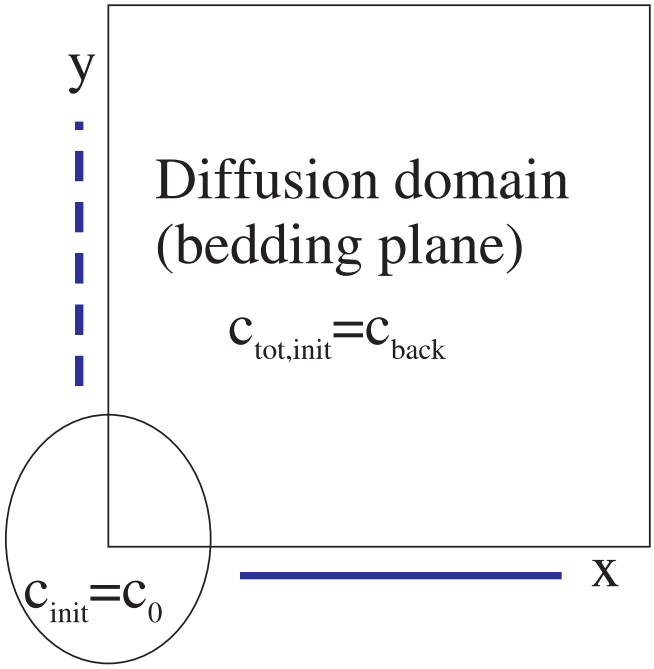

Fig. 3. Schematic representation of the geometry of the model. The calculation domain corresponds to a bedding plane and the borehole (area enclosed by the square). The trace of the borehole is not cylindrical due to the 45° angle between bedding and borehole. The solid and dashed lines parallel to the x and y axes make reference to the orientations of the tracer profiles shown in Fig. 4.1. The profiles corresponding to the dashed line were not taken following a bedding plane. Those tracer profiles were projected onto the bedding plane for comparison with model results.

The results obtained from the field experiment were compared with through-diffusion data measured in the laboratory for diffusion parallel to the bedding [11]. Because the measurements were performed at 23 °C, the diffusion coefficients had to be corrected for temperature before comparing them with the field data, which were obtained at 14 °C. When the diffusion coefficient at a given temperature T_1 is known ($D_{\mathrm{e}}^{T_1}$) its value at a temperature T_2 can be calculated by the following equation:

$$D_{\mathrm{e}}^{T_2} = D_{\mathrm{e}}^{T_1}\, \mathrm{e}^{\frac{E_{\mathrm{a}}}{R}\left(\frac{1}{T_1}-\frac{1}{T_2}\right)} \tag{3}$$

with E_{a} = activation energy for diffusion [$\mathrm{J\,mol^{-1}}$] and R = gas constant [8.314 $\mathrm{J\,mol^{-1}\,K^{-1}}$]. The activation energy for diffusion of HTO in Opalinus Clay from Mont Terri was 20 $\mathrm{kJ\,mol^{-1}}$. For $^{22}Na^+$ and $^{36}Cl^-$, a value of $E_{\mathrm{a}} = 18.8\,\mathrm{kJ\,mol^{-1}}$ was found [17]. The values of D_{e} at 14 °C, as calculated with Eq. (3), were a factor of 1.3 lower than those measured at 23 °C.

3.2.1 HTO

HTO is a non-sorbing tracer and is used to measure the transport properties of water. The best agreement between model calculations and experimental results was obtained using $D_e = 4 \times 10^{-11}$ m^2/s and $\phi = 0.15$ (Fig. 4.1). These values are very similar to the parameters obtained from laboratory through-diffusion experiments [11] and corrected for temperature: $D_e = (4.2 \pm 0.4) \times 10^{-11}$ m^2/s, $\phi = 0.17 \pm 0.02$. Notice, also, that the first measured points in the profiles, closest to the borehole, are slightly anomalous. The measured effective diffusion coefficient is in good agreement with the value of 5×10^{-11} m^2/s measured by Palut *et al.* [9] in a similar *in situ* diffusion experiment in the Mont Terri URL. Unlike in this study, Palut *et al.* [9] could observe two different zones: a disturbed zone close to the borehole wall with a higher diffusion coefficient, and a second undisturbed zone with a lower diffusion coefficient (5×10^{-11} m^2/s).

3.2.2 Iodide

I^- has been assumed to be non-sorbing. The idea of using iodide as tracer was to investigate possible anion-exclusion effects. The best agreement between model calculations and experimental results was obtained using $D_e = 1 \times 10^{-11}$ m^2/s and $\phi = 0.085$ (Fig. 4.2). Notice however that the first measured points in the profiles, closest to the borehole, are anomalous. This anomaly is even more pronounced than in the HTO profiles.

Two different sets of iodide profiles can be observed in Fig. 4.2b. First, iodide concentrations in the pore water are calculated from the experimental data using the measured water content, *i.e.*, the total water-filled porosity. Water-content porosities, calculated from gravimetric water contents, range from 0.14 to 0.17 (one of the profiles, corresponding to a small sandy layer, displays smaller water contents). Dividing these concentrations by a factor of 0.6, a good agreement between model and experimental results is achieved. This factor of 0.6 is equivalent to assuming that only 60% of the water-content porosity is accessible to iodide, *i.e.*, the accessible porosity for iodide ranges between 0.08 and 0.10. The value used in the model calculations ($\phi = 0.085$) is within this range.

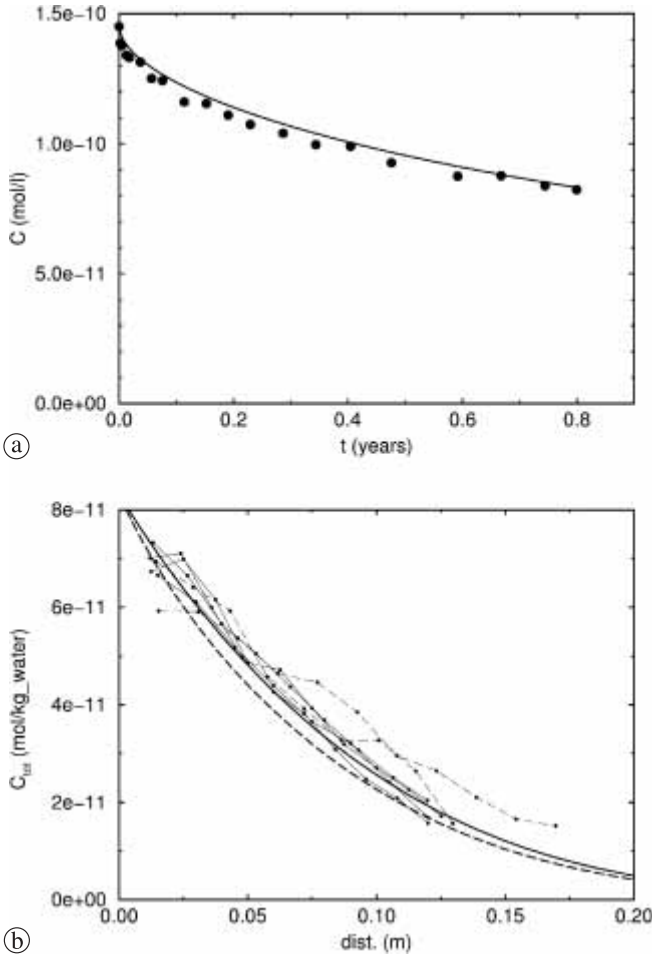

Fig. 4.1. Results for HTO. Model parameters: $D_e = 4 \times 10^{-11}$ m^2/s, $\phi = 0.15$. (**a**) Concentration in the injection system *vs*. time. The dots are experimental data; the line represents model calculations. (**b**) Tracer profiles in the rock (total concentration *vs*. distance from borehole wall). Thick lines correspond to model results; thin lines correspond to experimental data. Dashed lines correspond to the profiles that were not taken following a bedding plane (experimental data have been projected onto a bedding plane for comparison with model results).

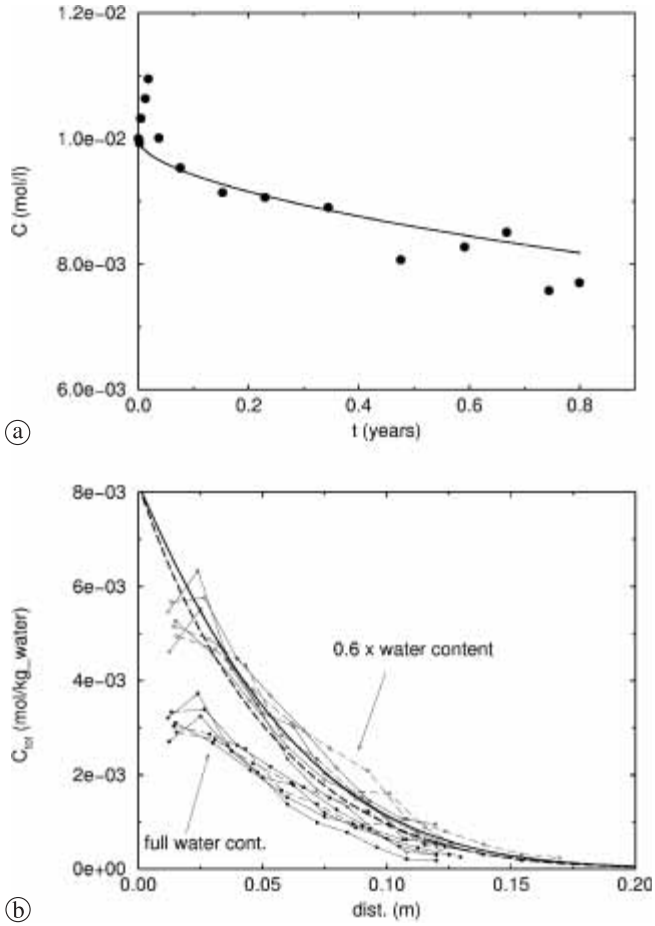

Fig. 4.2. Results for I^-. Model parameters: $D_e = 1 \times 10^{-11}$ m^2/s, $\phi = 0.085$. (**a**) Concentration in the injection system *vs*. time. The dots are experimental data; the line represents model calculations. (**b**) Tracer profiles in the rock (total concentration *vs*. distance from borehole wall). Thick lines correspond to model results; thin lines correspond to experimental data. Dashed lines correspond to the profiles that were not taken following a bedding plane (experimental data have been projected onto a bedding plane for comparison with model results). Two sets of profiles, calculated with different water contents, are shown (see text for explanation).

The values obtained are in very good agreement with the results for Cl^- from through-diffusion experiments [11] and corrected for temperature: $D_e = (1.3 \pm 0.1) \times 10^{-11}\,m^2/s$, $\phi = 0.08 \pm 0.01$. There is also a good agreement with another *in situ* diffusion experiment [10]. The effective diffusion coefficient for I^- found in that study was $1.5 \times 10^{-11}\,m^2/s$.

3.2.3 Sodium

Na^+ is a weakly-sorbing cation. The results of through-diffusion experiments (this study) have shown that the sorption of trace amounts of $^{22}Na^+$ in Opalinus Clay can be described with a linear sorption model. The best agreement between model calculations and experimental results was obtained using $D_e = 6 \times 10^{-11}\,m^2/s$ and a rock capacity factor α equal to 0.64 (Fig. 4.3). This value of α has been implemented in the model by using a porosity of 0.17 and a distribution coefficient K_d equal to 0.21 l/kg. These values are in very good agreement with the results from through-diffusion experiments [11] and corrected for temperature: $D_e = (5.7 \pm 0.5) \times 10^{-11}\,m^2/s$, $\phi = 0.62 \pm 0.05$.

3.2.4 Caesium

Cs^+ is a strongly sorbing cation. There are no experimental data available for the transport properties of Cs^+ in Opalinus Clay. However, there have been sorption studies. Lauber *et al.* [18] performed batch sorption experiments with Opalinus Clay samples and synthetic Opalinus Clay pore water and were able to describe the sorption of Cs^+ by means of a Freundlich isotherm ($s = 0.372c^{0.53}$). In principle, since the initial concentration of Cs^+ in the experiment (10^{-3} mol/l) is small compared to the salinity of the Opalinus Clay pore water, it could be argued that this isotherm could be applied to the case of the field experiment. However, a good fit to both the evolution of the tracer in the injection system and the profiles in the rock could not be obtained with this isotherm.

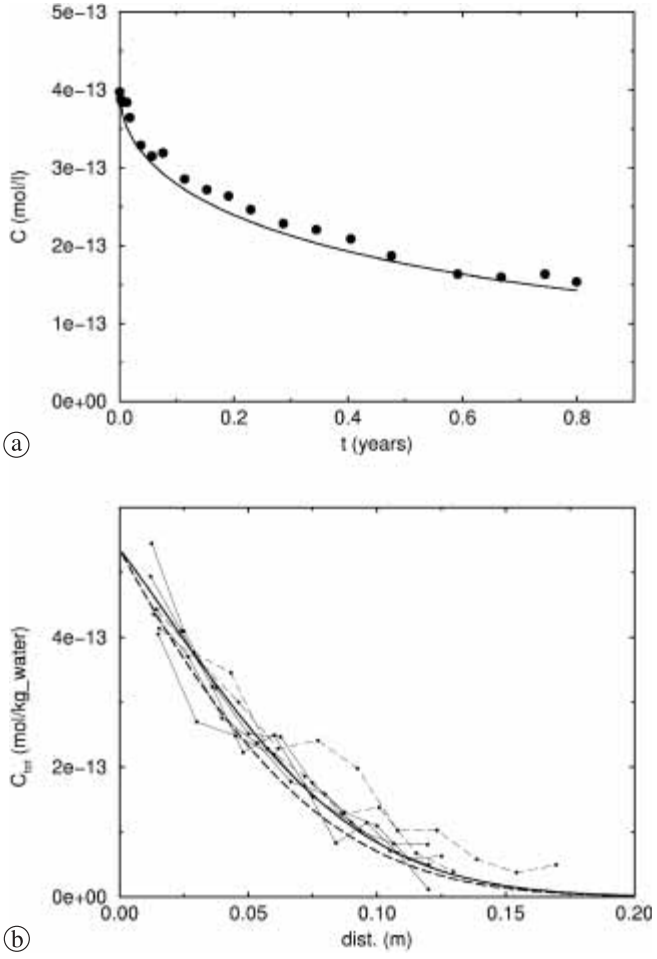

Fig. 4.3. Results for $^{22}Na^+$. Model parameters: $D_e = 6 \times 10^{-11}\,m^2/s$, $\alpha = 0.64$ ($\phi = 0.17$, $K_d = 0.21$ l/kg). (**a**) Concentration in the injection system *vs*. time. The dots are experimental data; the line represents model calculations. (**b**) Tracer profiles in the rock (total concentration *vs*. distance from borehole wall). Thick lines correspond to model results; thin lines correspond to experimental data. Dashed lines correspond to the profiles that were not taken following a bedding plane (experimental data have been projected onto a bedding plane for comparison with model results).

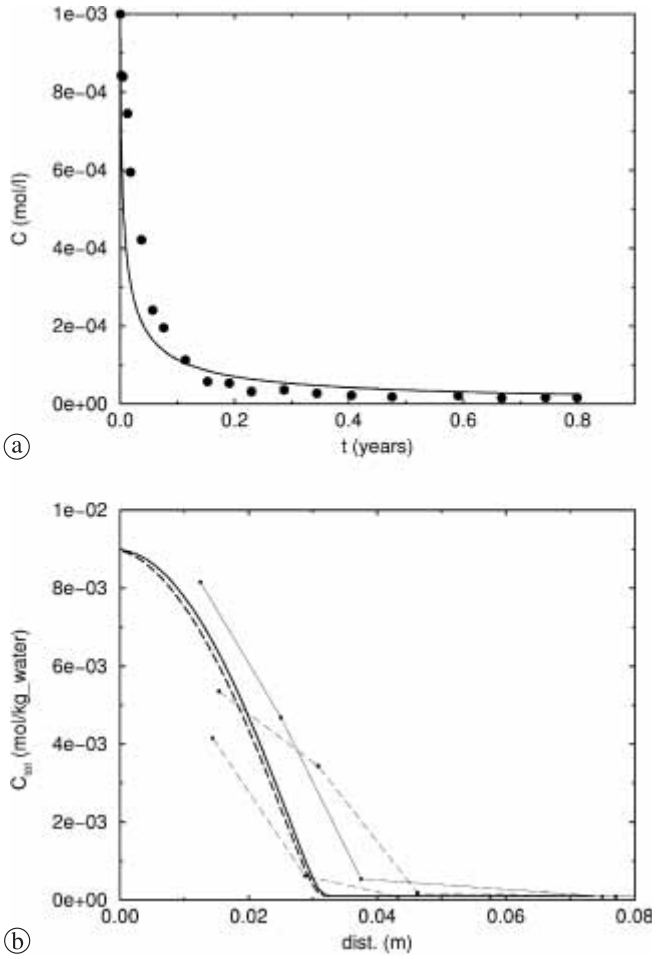

Fig. 4.4. Results for Cs^+. Model parameters: $D_e = 2 \times 10^{-10}\,m^2/s$, $\phi = 0.17$, $s = 0.186c^{0.53}$. (**a**) Concentration in the injection system *vs*. time. The dots are experimental data; the line represents model calculations. (**b**) Tracer profiles in the rock (total concentration *vs*. distance from borehole wall). Thick lines correspond to model results; thin lines correspond to experimental data. Dashed lines correspond to the profiles that were not taken following a bedding plane (experimental data have been projected onto a bedding plane for comparison with model results).

An approximate fit could be obtained using the isotherm $s = 0.186c^{0.53}$, which is equivalent to the isotherm proposed by Lauber *et al.* [18] divided by 2, and an effective diffusion coefficient D_e equal to 2×10^{-10} m^2/s (Fig. 4.4).

The comparison between modelling and experimental results suggests an "upscaling" effect from batch sorption studies (clay suspensions in solution) to field conditions (intact rock) leading to a slight decrease in sorption capacity of the rock matrix. Regarding the transport properties, the obtained effective diffusion coefficient is about a factor of 5 larger than the effective diffusion coefficient for water (HTO). This is in qualitative agreement with recent through diffusion data on samples from the Callovo–Oxfordian clay [19], which indicate significantly higher D_e values for Cs^+ relative to HTO.

4. Conclusions

The *in situ* diffusion of HTO, I^-, $^{22}Na^+$ and Cs^+ in Opalinus Clay was studied in the Mont Terri Underground Rock Laboratory by injecting a cocktail in a single borehole. Effective diffusion coefficients and rock capacity factors (porosity values) were calculated from the decrease of tracer concentration in the borehole and from the tracer profiles in the surrounding rock. Diffusion was found to occur mainly parallel to the bedding of the rock. The diffusion coefficients and rock capacity factors for HTO, iodide and sodium obtained from the field measurements were in excellent agreement with those determined in through-diffusion experiments in the laboratory. No evidence for an excavated disturbed zone (EDZ) was found from the diffusion behaviour of the tracers.

In the case of caesium no laboratory measurements are currently available to confirm obtained diffusion data. However, the high effective diffusivity is in qualitative agreement with recent through-diffusion data on samples from the Callovo–Oxfordian clay which indicate significantly higher D_e values for Cs^+ relative to HTO. The reason for this is currently not understood.

The *in-situ* experiment is a first step in an upscaling process. Both the diffusion path length, as well as the diffusion time were increased by a factor of 10 in the case of HTO, I^- and $^{22}Na^+$. For Cs^+, the diffusion time was too short to cover a large diffusion distance.

These first results are encouraging and indicate that lab diffusion data can be used with confidence to assess diffusion on larger distances over longer time periods.

Acknowledgment. We would like to express our thanks to Bart Baeyens (PSI) for performing the Cs extractions. Further we thank Thomas Fierz (Solexperts) for the technical layout and monitoring of the *in-situ* experiment and Heinz Steiger (Geotechnical Institute) for sampling and monitoring. The overcoring was planned and managed by Andreas Möri and Paul Bossart (Geotechnical Institute). The drilling was carried out by COREIS (France). The authors also thank Rolf Gloor, Martin Casanova (Bachema) and Claude Aubry (OEPN) for the chemical analysis.

References

1. Ondraf/Niras: Technical overview of the SAFIR 2 report. Technical Report NIROND 2001-05 E, Brussels, Belgium (2001).
2. Nagra: Project Opalinus Clay: Safety Report – Demonstration of disposal feasibility for spent fuel, vitrified high-level waste and long-lived intermediate-level waste (Entsorgungsnachweis). Nagra Technical Report NTB-02-05, Nagra, Wettingen, Switzerland (2002).
3. Andra: Dossier 2001 Argile. Progress report on feasibility studies & research into deep geological disposal of high-level, long-lived waste. Synthesis report. Andra, Paris, France (2001).
4. Van Loon. L. R., Soler, J. M., Bradbury, M. H.: Diffusion of HTO, $^{36}Cl^-$ and $^{125}I^-$ in Opalinus Clay samples from Mont Terri. Effect of confining pressure. J. Contam. Hydrol. **61**, 73 (2003).
5. Van Loon, L. R., Soler, J. M., Jakob, A., Bradbury, M. H.: Effect of confining pressure on the diffusion of HTO, $^{36}Cl^-$ and $^{125}I^-$ in a layered argillaceous rock (Opalinus Clay): diffusion perpendicular to the fabric. Appl. Geochem. **18**, 1653 (2003).
6. Tevissen, E., Soler, J. M.: *In-situ* diffusion experiment (DI): Synthesis Report. Mont Terri Project, Technical Report TR2001-05 (2003).
7. Degueldre, C., Scholtis, A., Laube, A., Turrero, M. J., Thomas, B.: Study of the pore water chemistry through an argillaceous formation: a paleohydrochemical approach. Appl. Geochem. **18**, 55 (2003).
8. Rübel, A. P., Sonntag, C., Lippmann, J., Pearson, F. J., Gautschi, A.: Solute transport in formations of very low permeability: Profiles of stable isotope and dissolved gas contents of pore water in the Opalinus Clay, Mont Terri, Switzerland. Geochim. Cosmochim. Acta **66**, 1311 (2002).
9. Palut, J.-M., Montarnal, Ph., Gautschi, A., Tevissen, E., Mouche, M.: Characterisation of HTO diffusion properties by an *in situ* tracer experiment in Opalinus Clay at Mont Terri. J. Contam. Hydrol. **61**, 203 (2003).
10. Tevissen, E., Soler, M. J., Montarnal, P., Gautschi, A., Van Loon, L. R.: Comparison between *in situ* and laboratory diffusion studies of HTO and halides in Opalinus Clay from the Mont Terri. Radiochim. Acta **92**, 781 (2004).
11. Van Loon, L. R., Soler, J. M., Müller, W., Bradbury, M. H.: Anisotropic diffusion in layered argillaceous formations: a case study with Opalinus clay. Environ. Sci. Technol. (2004), in press.
12. Wersin, P., Van Loon, L. R., Soler, J. M., Yllera, A., Eikenberg, J., Gimmi, Th., Hernán, P., Boisson, J.-Y.: Long-term diffusion experiment at Mont Terri: first results from field and laboratory data. Appl. Clay Sci. **26**, 123 (2004).
13. Pearson, F. J.: Opalinus clay experimental water: A1 Type, Version 980318. Internal Technical Report TM-44-98-07, Paul Scherrer Institut, Villigen PSI, Switzerland (1998).
14. Möri, A., Inderbitzin, L., Nussbaum, C., Eikenberg, J., Rüthi, M., Aubry, C., Brisset, N., Steiger, H., Bossart, P.: Long-term diffusion (DI-A) – Sampling documentation of BDI-A1 OC Borehole. Mont Terri Project, Technical Note 2003-20 (2003).
15. Steefel, C. I.: GIMRT, Version 1.2: Software for Modeling Multicomponent, Multidimensional Reactive Transport. User's Guide, UCRL-MA-143182. Lawrence Livermore National Laboratory, Livermore, California (2001).
16. Steefel, C. I., Yabusaki, S. B.: OS3D/GIMRT, Software for Multicomponent-Multidimensional Reactive Transport. User's Manual and Programmer's Guide. PNL-11166, Pacific Northwest National Laboratory, Richland, Washington (1996).
17. Van Loon, L. R., Müller, W., Iijima, K.: Activation energy of the self-diffusion of HTO, $^{22}Na^+$ and $^{36}Cl^-$ in a highly compacted argillaceous rock (Opalinus Clay). Submitted for publication in Appl. Geochem. (2004).
18. Lauber, M., Baeyens, B., Bradbury, M. H.: Physico-Chemical Characterisation and Sorption Measurements of Cs, Sr, Ni, Eu, Th, Sn aand Se on Opalinus Clay from Mont Terri. PSI Technical Report Nr. 00-10, Paul Scherrer Institut, Villigen, Switzerland (2000).
19. Tevissen, E.: Personal communication (2003).